This article has been accepted for publication in a future issue of this journal, but has not been fully edited. Content may change prior to final publication. Citation information: DOI 10.1109/JLT.2018.2883541, Journal of Lightwave Technology

Nonlinearity-free Coherent Transmission in Hollow-Core Antiresonant Fiber

Zhixin Liu[1] *Senior Member, IEEE,* Boris Karanov[1], *Student Member, IEEE* Lidia Galdino[1], *Member, IEEE,* John R. Hayes[2], Domaniç Lavery[1], *Member, IEEE,* Kari Clark[1], Kai Shi[1], *Member, IEEE,* Daniel J. Elson[1], Benn C. Thomsen[1], *Member, IEEE,* Marco N. Petrovich[2], *Senior Member, IEEE,* David J. Richardson[2], *Fellow, IEEE,* Francesco Poletti[2], *Member, IEEE,* Radan Slavík[2], *Senior Member, IEEE,* and Polina Bayvel[1], *Fellow, IEEE*

***Abstract*—We demonstrate the first multi-terabit/s WDM data transmission through hollow-core antiresonant fiber (HC-ARF). 16 channels of 32-GBd dual-polarization (DP) Nyquist-shaped 256QAM signal channels were transmitted through a 270-m long fiber without observing any power penalty. In a single-channel high power transmission experiment, no nonlinearity penalty was observed for up to 1 W of received power, despite the very low chromatic dispersion of the fiber (<2 ps/nm/km). Our simulations show that such a low level of nonlinearity should enable transmission at 6.4 Tb/s over 1200 km of HC-ARF, even when the fiber attenuation is significantly greater than that of SMF-28. As signals propagate through hollow-core fibers at close to the speed of light in vacuum such a link would be of interest in latency-sensitive data transmission applications.**

***Index Terms*— Optical fiber communication, Coherent transmission, Fiber nonlinearity, Modulation, Hollow-core Antiresonant Fiber.**

I. Introduction

DRIVEN by the continual succession of new applications and technologies the information transfer capacity of optical communication networks has grown exponentially over several decades, transforming almost every aspect of the global economy and our everyday social lives. This transformative power has come about as a result of many technological breakthroughs including the development of low-loss, single mode transmission fiber (SMF), the erbium-doped fiber amplifier (EDFA), wavelength division multiplexing (WDM), and more recently digital signal processing (DSP) enabled coherent transmission. Throughout this technological evolution, silica-based single mode optical fiber has remained at the heart of optical communication networks. Spectacular as it is impact has been, the silica optical fiber has its weakness: the Kerr nonlinearity. This ultimately degrades the quality of propagating optical signals and limits the maximum information transmission capacity. This in turn has the potential to result in a "capacity crunch" at various points in the global optical communication network [1].

In addition to traditional data transfer, new data hungry services such as machine-to-machine communications inside data centers (DCs), 5G mobile communications, and the Internet of Things are starting to dominate the network traffic. These new services place further requirements on the data transfer performance, in particular with regards to transmission latency within the network. For example, data center operators have recently specified a maximum round-trip time of less than 2.0 ms for metro inter-DC communication [2]. Emerging applications such as virtual reality, the tactile internet, and autonomous driving will impose even more stringent requirements on the maximum allowed latency, with stability of latency also now becoming an important consideration in many instances. [3].

The intrinsic problems of silica fiber (nonlinearity and latency), have triggered numerous research activities, ranging from hardware technologies through to software DSP algorithms. On the mitigation of nonlinearity-induced impairments front, digital impairment compensation techniques including digital backward propagation [4] and the nonlinear Fourier transform [5] have attracted significant research interest as they can be employed with no/ minimal changes to currently deployed fiber links. Nevertheless, they are intrinsically limited by the bandwidths and resolutions available for coherent receivers. Optical phase conjugation (OPC) promises simultaneous compensation of both dispersion and nonlinearity at the expense of building symmetric transmission links [6]. Phase sensitive amplification (PSA) can in principle achieve noise-less amplification and can even be used to regenerate signal constellations. However, it is challenging to implement PSA for wide bandwidth WDM signals and requires precise control of chromatic dispersion [7, 8]. Effective as the above-mentioned technologies are, they can only mitigate nonlinearity impairments, not eliminate them.

In optical networks, especially in long-reach transmission systems, the data transmission delay is dominated by signal

Manuscript received xxx, 2018; revised xxx; accepted xxx. Date of publication xxx; date of current version xxx. This work was supported by the U.K. Engineering and Physical Sciences Research Council under Grant EP/P030181/1 (AirGuide Photonics), EP/R041792/1 and EP/R035342/1 (TRANSNET). Royal Society RSG\R1\180200. EU Marie Skłodowska-Curie COIN (grant No. 676448)

Z. Liu, B. Karanov, L. Galdino, D. Lavery, K. Clark, D. J. Elson, K. Shi, B. C. Thomsen, and P. Bayvel are with the Department of Electronics and Electrical Engineering, University College London, London, WC1E 7JE, U.K. (e-mail: zhixin.liu@ucl.ac.uk; boris.karanov.16@ucl.ac.uk; l.galdino@ucl.ac.uk; d.lavery@ucl.ac.uk; p.bayvel@ucl.ac.uk).

J. R. Hayes, M. N. Petrovich, D. J. Richardson, F. Poletti, R. Slavík are with the Optoelectronics Research Centre, University of Southampton, Southampton SO17 1BJ, U.K. (e-mail: jrh1@soton.ac.uk; nmp@orc.soton.ac.uk; djr@orc.ucl.ac.uk; fp@soton.ac.uk; R.Slavik@soton.ac.uk).

This work is licensed under a Creative Commons Attribution 3.0 License. For more information, see http://creativecommons.org/licenses/by/3.0/.

This article has been accepted for publication in a future issue of this journal, but has not been fully edited. Content may change prior to final publication. Citation information: DOI 10.1109/JLT.2018.2883541, Journal of Lightwave Technology

propagation in the optical fibers [9]. For this reason, network operators are increasingly looking to deploy low latency systems by installing as straight as possible fiber links between sites to support financial and other high value latency sensitive applications [10]. Researchers are also investigating new solid fiber designs for low latency transmission and a 0.3% reduction in propagation latency has been obtained by engineering/optimizing the design of solid core silica fiber [11].

By contrast hollow-core fibers (HCF)s exhibit ~30% reduction of latency, a high damage threshold and more than three orders of magnitude lower nonlinear response than standard silica optical fiber. Such a combination of advantages over conventional solid-core silica fiber make them an exciting option to meet both the emerging capacity and latency needs in future optical networks [12, 13].

Broadly speaking, there are two classes of hollow-core fiber: hollow-core photonic bandgap fiber (HC-PBGF) and hollow-core antiresonant fiber (HC-ARF). The HC-PBGF guides light in a hollow core by virtue of photonic bandgap effects determined by a carefully designed glass microstructure [14]. The HC-ARFs, however, rely essentially on coherent reflections from thin and typically tubular glass membranes to confine and guide light in the hollow region [15-19]. These membranes behave effectively as Fabry-Perot type resonators, with their transmission signature consisting of sharp peaks (resonances) separated by high reflectivity regions referred to as antiresonance windows. Within these windows, the grazing incidence provided by the large hollow-core results in very high reflectivity for the membranes, and translates into orders of magnitude lower leakage loss. These fibers offer the flexibility of engineering low-loss transmission windows simply through the choice of membrane thickness, and numerical simulations are currently indicating that they can provide lower attenuation than almost any existing fibers at almost any wavelength [19].

To date, a significant body of work has been done to demonstrate transmission in hollow-core photonic bandgap fibers, with both high capacity (73.7 Tb/s) [20] and relatively long lengths (up to 74.8 km) in a re-circulating loop demonstrated [21]. However, for HC-ARF, only single-channel 10-Gb/s on-off keyed (OOK) signal transmission over a fiber length of just 100 m has been demonstrated [15]. Compared to HC-PBGF, the key advantages of HC-ARF include an ultra-large transmission window (for example, a 1100 nm wide transmission bandwidth as shown in ref. [15]) with almost constant mode field diameter and a very high differential modal loss (>10 times higher loss in high order modes than the fundamental mode) that effectively supports single-mode transmission. Moreover, theoretical studies have identified a potential low loss (<0.15 dB/km) and a very low chromatic dispersion (CD) over almost the entire transmission window (<2 ps/(nm·km)) [20]. This potential is supported by a recent demonstration of a 0.5 km length HC-ARF with a loss of 1.3 dB/km [22], outperforming the lowest rigorously documented loss in a HC-PBGF (1.7 dB/km) [23]. Arguably the key potential advantage of HC-ARF lies in the potential for very high transmission capacities using wide wavelength range dense wavelength division multiplexing (DWDM) and high-order modulation formats due to the anticipated very high nonlinearity tolerance. Although the prior art in [15] showed that the HC-ARF has a broad transmission window, its capability of supporting DWDM transmission (e.g. no wavelength-dependent fading or transmission impairments) has not been confirmed. Further, no study of nonlinear transmission impairments in HC-ARF has been reported to date.

In this paper, we show the significant potential of HC-ARF for optical communications by demonstrating the coherent transmission of a very high-order modulation format (256QAM) signal, over two polarizations, in a 16-channel 32 GBd DWDM system. This results in a >14 times greater spectral efficiency (14.5 bit/s/Hz) than the previous demonstration, over a 2.7 time longer (270 m) length of HC-ARF. Importantly, we demonstrate for the first time the high tolerance to nonlinearities in HC-ARF relative to SMF-28 in coherent transmission. These experiments were first reported at OFC 2017 [24]. This paper extends the conference abstract by showing the superior nonlinearity tolerance of HC-ARF relative to SMF-28 (even in experimental conditions that are deliberately biased against the HC-ARF). Moreover, through simulation, we compare the nonlinear tolerance HC-ARF to SMF-28 and large effective area solid core fibers, and investigate the potential of using HC-ARF in a 1200-km long low latency coherent communication system. Experimental characterization of the CD of the fiber is shown for the first time, essentially confirming the low values of CD predicted in [15].

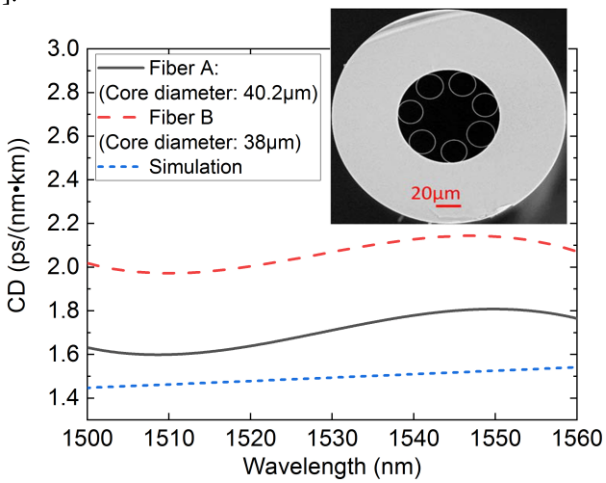

Fig. 1. Measured chromatic dispersion. Fiber A: solid black line; Fiber B: dashed red line; Simulation: dotted blue line.

II. Low Dispersion Antiresonant Fiber

The two HC-ARF fibers in this work were drawn from the same cane and have a non-contacting tubular geometry with seven tubes around a hollow core, as shown in the inset in Fig. 1. Their loss characterization and simulated dispersion were previously reported in [15]. Here, we experimentally measure the CD of the two fibers using the RF phase shift method [25] employing a tunable laser (1500 to 1585 nm) with a step size of 0.1 nm. The measured group delay was converted to CD using a 5-term Sellmeier fit to each raw group delay trace [26]. This

This work is licensed under a Creative Commons Attribution 3.0 License. For more information, see http://creativecommons.org/licenses/by/3.0/.

This article has been accepted for publication in a future issue of this journal, but has not been fully edited. Content may change prior to final publication. Citation information: DOI 10.1109/JLT.2018.2883541, Journal of Lightwave Technology

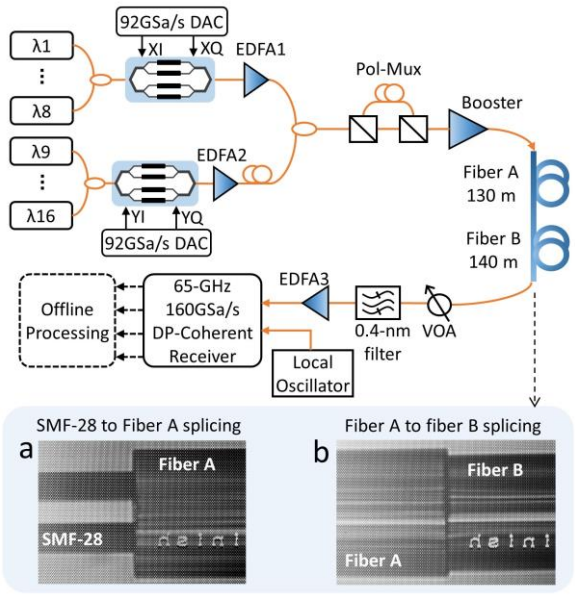

Fig. 2 Experimental setup for WDM transmission. EDFA: erbium-doped fiber amplifier; DAC: digital-to-analog converter; VOA: variable optical attenuator.

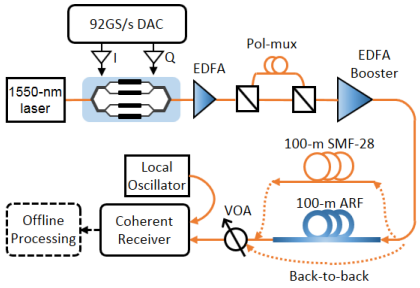

Fig. 3 Experimental setup for single-channel high power transmission.

measurement system allowed for an accurate CD measurement with a resolution of 0.1 ps/(nm•km). The solid and dashed lines in Fig. 1 show the measured CD for fiber A and fiber B, with core diameters of 38 and 40.2 μm, respectively. The dotted line shows the simulation result reported in [15] for comparison. The measured CD is slightly higher than the simulation results but a very low and flat dispersion is obtained across the full measurement wavelength range. The average CD for fiber A and fiber B was 2.0 and 1.7 ps/(nm•km), respectively.

An important benefit comes with the low dispersion of HC-ARFs is the reduction of DSP complexity. For example, the number of taps for a 1200 km transmission system with SMF-28 requires 167 taps (assuming CD of 17 ps/(nm.km)), whereas only 19 taps (assuming CD of 2 ps/(nm.km)) is needed when using HC-ARF [27]. This means that coherent system can eliminate the use of static equalizers for CD compensation, thereby reducing both the DSP complexity and processing delay.

III. Transmission Experiment

Fig. 2 shows the experimental set-up of our WDM transmission experiment. The DWDM transmitter consists of 16 tunable external cavity lasers (ECLs， linewidth of 100 kHz) spaced between 1544.13 nm and 1550.12 nm on a 50-GHz ITU grid. The odd (and even) channels were combined through an 8×1 coupler and subsequently modulated with a $LiNbO_3$ IQ modulator driven by two 92-GS/s digital-to-analog convertors (DACs). The modulated odd and even channels were amplified and decorrelated before being combined and passed through a polarization multiplexing emulation stage to form a 16-channel 32 GBd dual-polarization (DP) 256QAM signal. The power of each ECL was adjusted to yield a flat DWDM power spectrum (with less than 1 dB power variation) after the high-power EDFA. The high-power EDFA boosted the total signal power to 35 dBm (3.5 W), corresponding to 23 dBm per channel. The amplified signal was then launched into the HC-ARF transmission link via a SMF-28 to HC-ARF splice connection with a loss of 3.5 dB (due to the significant mode field mismatch) – see inset (a) in Fig. 2. The HC-ARF link comprised the two longest HC-ARF spans available, which were spliced together (inset Fig. 2b) to enable a transmission distance of 270 m. The first span (fiber A) is 130 m long and has a 40 μm core and a 200 μm cladding diameters. The second span (fiber B) is 140 m long and has a 38 μm core and a 170 μm cladding diameters. Their transmission performance were previously reported in [15]. Over the C-band it has an average loss of 41 dB/km. The second span is 140 m long and has a 38 μm core and a 180 μm cladding diameter. Its loss over the C-band is 58 dB/km. After transmission, the signal was coupled back from the HC-ARF to SMF-28 with a ~ 4-dB loss.

The average loss of the line at the transmission wavelength region was approximately 21.5 dB, including 14 dB fiber loss and 7.5 dB coupling loss. A lower HCF to SMF-28 coupling loss could be achieved by using a mode field diameter matching buffer fiber [28], unfortunately though such a buffer fiber was not available for this experiment. The channel of interest was selected by passing the DWDM signal through a 50-GHz flat-top optical filter and was subsequently pre-amplified (EDFA3) and detected using a 65-GHz dual-polarization coherent receiver. The local oscillator (LO) laser was a 100-kHz-linewidth tunable ECL and the detected signals were then sent to four 160 GSa/s analog-to-digital convertors (ADCs) for offline signal demodulation. In order to compare the result with the back-to-back performance at the same optical signal-to-noise ratio (OSNR), the fiber link was replaced with a variable optical attenuator (VOA) to emulate the loss.

The multi-level drive signals required for the QAM format were generated from decorrelated pseudorandom binary sequences (PRBSs) of length 2^{16}. The transmitter-side DSP shaped the generated QAM signal using a root raised-cosine (RRC) filter with a roll-off factor of 1% to generate the 32 GBd Nyquist-shaped 256QAM signals. At the receiver side, the signal was down sampled to 2 Sa/sym before equalizing the digital signals using a 21-tap blind radially directed equalizer for polarization demultiplexing. The carrier-frequency offset and phase noise were compensated with conventional DSP algorithms as described in [29]. The demodulated symbols were used to calculate the bit error rate (BER) and signal-to-noise ratio (SNR).

In addition to the WDM experiment, we investigated the high-power, single-channel performance of a length of HC-ARF, in order to enable us to compare the nonlinearity-induced

This work is licensed under a Creative Commons Attribution 3.0 License. For more information, see http://creativecommons.org/licenses/by/3.0/.

This article has been accepted for publication in a future issue of this journal, but has not been fully edited. Content may change prior to final publication. Citation information: DOI 10.1109/JLT.2018.2883541, Journal of Lightwave Technology

transmission penalties of HC-ARF with respect to conventional SMF-28. As shown in Fig. 3, the experimental setup for the single channel transmission was the same as the WDM

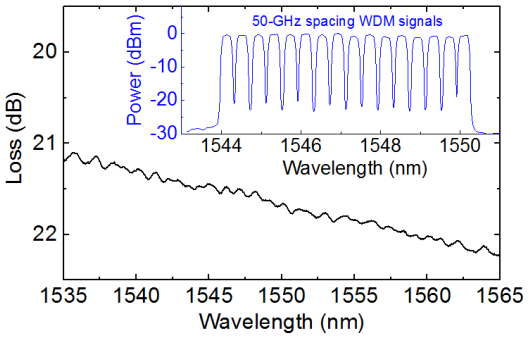

Fig. 4 The loss profile of the 270-m HC-ARF fiber link (black line) and spectrum of the transmitted WDM signals (blue line), measured using an OSA with a resolution of 0.1 nm.

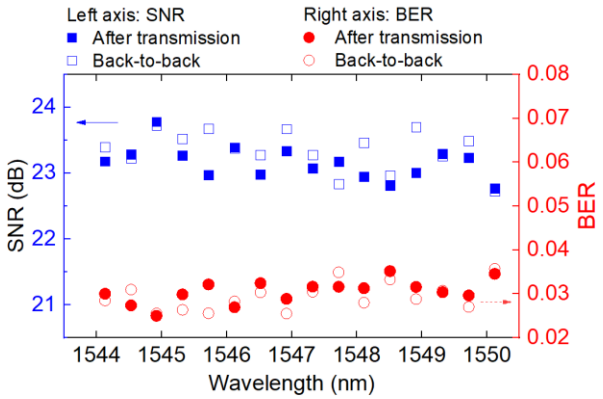

Fig. 5 Measured SNR (square marker) and BER (circle marker) both back-to-back (open marker) and after transmission (closed maker) though the 270-m HC-ARF fiber link.

experiment except that only one ECL at 1550.12 nm was used and the 270 m HC-ARF link was replaced with 100 m HC-ARF (the lowest loss sample available, with an attenuation of 40 dB/km) and a 100 m length of SMF-28. Due to the loss in the HC-ARF sample (about 4 dB) as compared to the negligible loss in SMF-28 of the same length, it is difficult to decide at which power to carry out the comparison of nonlinear impairments. However, we decided to show the impact of nonlinearity impairment with reference to the optical power after transmission, meaning that the local power along the HC-ARF length is always higher than the power along at the equivalent point in the SMF-28. This biases the comparison in favor of the SMF-28. Limited by the maximum output power (36.5 dBm) of our high-power EDFA and the 3.5 dB input coupling loss from SMF-28 to the HC-ARF, the maximum launch power into the HC-ARF was 32.5 dBm (measured at the input of the HC-ARF), resulting in 28.5 dBm power after HC-ARF transmission. The performance of the signal was compared to an SMF-28 transmission with 28.5 dBm launch power, as plotted in Fig. 6.

IV. Experimental Results

A. WDM transmission

Fig. 4 shows the measured loss profile of the HC-ARF link and the optical spectrum of the transmitted WDM signal. The total link loss within the C-band increases smoothly from 21.2 dB to 22.2 dB for wavelengths from 1535 nm to 1565 nm. Fig. 5

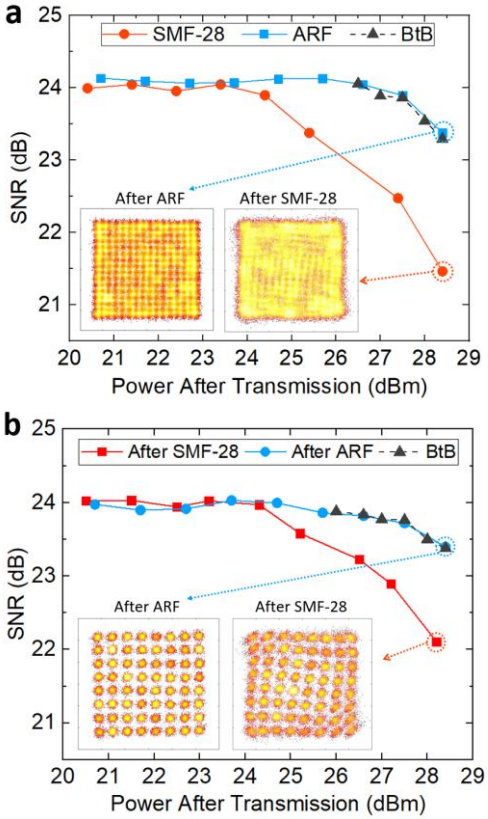

Fig. 6. SNR of the single-carrier (a) DP-256QAM and (b) DP-64QAM transmission over 100-m HC-ARF (blue square marker), 100-m SMF-28 (red circle marker), and back-to-back (black triangle marker); Constellation diagrams at the power of 28.5dBm after HC-ARF and SMF-28 transmission.

shows the SNRs and BERs of the transmitted WDM DP-256QAM signals over the 270 m HC-ARF link, as closed square and circle markers, respectively. The achieved SNR values ranged from 22.8 to 23.4 dB and the pre-FEC corresponding BER values ranged from 2.7×10^{-2} to 3.5×10^{-2}. Using soft-decision decoding with 17% overhead [29], we achieved error free transmission for all channels, yielding a net data rate of 6.8 Tb/s. The back-to-back results are shown as open markers in Fig. 5. The average SNR values for back-to-back and after transmission were 23.2 and 23.4 dB, respectively. We believe the slight difference in the SNR lies within the accuracy of our measurement.

B. High power single-channel transmission

Fig. 6 shows the SNRs of the transmitted single-channel 32 GBd DP-256QAM (Fig. 6a) and DP-64QAM (Fig. 6b) signals for various optical powers as measured at the output of the 100 m HC-ARF and the 100 m SMF-28, respectively. As mentioned earlier, this comparison is biased against HC-ARF as the optical power propagating in the HC-ARF is at all points higher than in the SMF-28. In Fig. 6 we can observe that the back-to-back performance degrades as the input power is increased above about 26 dBm. This is due to nonlinear impairments generated within the high-power EDFA, which was operated at output powers up to 36.5 dBm. The high-power

This work is licensed under a Creative Commons Attribution 3.0 License. For more information, see http://creativecommons.org/licenses/by/3.0/.

This article has been accepted for publication in a future issue of this journal, but has not been fully edited. Content may change prior to final publication. Citation information: DOI 10.1109/JLT.2018.2883541, Journal of Lightwave Technology

EDFA used was designed for CW operation and was not optimized for high power data signal amplification.

In the back-to-back case, the maximum achieved SNR was 24.2 dB due to the electronic noise limitations of the transceiver [30]. The SNR of the demodulated 256QAM signal remained about 24 dB before the post transmission power reached 26.5 dBm (corresponding to an EDFA output power of 34 dBm). The blue circle markers show the SNR obtained after transmission over the HC-ARF link. The performance was identical to the back-to-back case, confirming that no nonlinearity impairment occurred in the HC-ARF transmission. In contrast, SMF-28 fiber nonlinearity further degraded performance for post transmission powers above 25 dBm. The SNR of the demodulated signal dropped from 24.0 dB to 21.5 dB as the power was increased from 23.5 dBm to 28.5 dBm, corresponding to an increase in BERs from 2×10^{-2} to 5×10^{-2}.

The constellation diagrams corresponding to a transmission power of 28.5 dBm are shown as insets to Fig. 6. At 28.5 dBm, the SNR obtained after SMF-28 transmission was 2 dB lower than in the case of the HC-ARF transmission, highlighting the superior nonlinear tolerance of HC-ARF compared to SMF-28. A similar experiment was repeated for a single-channel 32 GBd DP-64QAM signal. The constellation diagrams in Fig. 6b clearly show the nonlinear phase distortion after 100 m SMF-28 transmission, while no significant distortion was observed after HC-ARF transmission even at the maximum post transmission power of 28.5 dBm.

The above results clearly evidenced that HC-ARFs have ultra low nonlinearity and the capability of handling very high optical powers. In HC-ARFs based optical communication systems, it is possible to launch high optical powers beyond the limitations of conventional SMF-28 based systems.

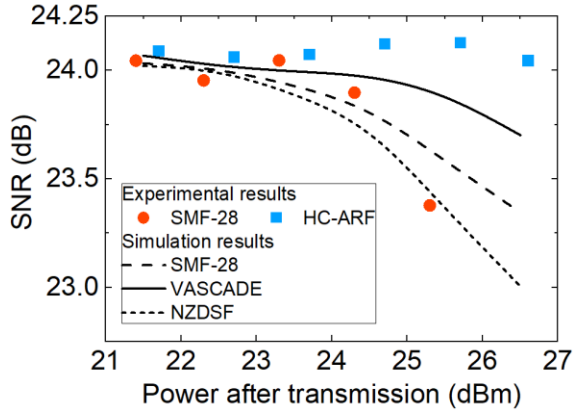

Fig. 7. Experimental and simulation results of the single-carrier 32-GBd DP-256QAM signal.

V. Simulation

A. Performance comparison of HC-ARF with different solid core fibers

We conducted simulations to compare the high HC-ARF nonlinearity tolerance to that of various types of commonly-used solid core fibers including large effective area solid core silica fiber and non-zero dispersion shifted fiber. We first simulated the transmission performance of 32 GBd DP-256QAM over a 100 m length of SMF-28 using the split step Fourier method with a step size of 1 m. By setting the transceiver noise limit to the experimentally-obtained value of 24.2 dB, the simulated SNR values at different optical powers showed good agreement with the experimental results (as shown by the dashed line in Fig. 7), which confirms the accuracy of our simulation. Subsequently, we changed the fiber parameters by assuming 100 m of Corning Vascade Ex3000 fiber (large effective area fiber) and non-zero dispersion shifted fiber (NZDSF), whose key parameters are listed in Table 1.

TABLE I
Fiber Parameters in Simulation

Parameters	SMF-28	Corning VASCADE EX3000 [31]	Corning non-zero dispersion shifted fiber [32]
Attenuation at 1550 nm (dB/km)	0.2	0.158	0.19
CD (ps/nm•km)	17	20.8	5
Effective area (μm^2)	80	150	72

The simulation results are plotted as lines (NZDSF: dotted; VASCADE: solid) in Fig. 7 together with the experimental results for SMF-28 (red circles) and HC-ARF (blue squares). Although the NZDSF fiber has a smaller dispersion, it underperforms compared to SMF-28 due to the smaller effective area. The simulation results show that the VASCADE fiber outperforms SMF-28 for optical powers higher than 23 dBm. However, the SNRs start to degrade as we further increase the power past 25 dBm, showing a 0.3 dB SNR penalty at 26.5 dBm. Similar to the experiment, this comparison is biased against the HC-ARF in that the optical power along the fiber is always higher than the solid core fibers, indicating that HC-ARF has a much higher nonlinearity tolerance than the state-of-the-art large effective area solid core fiber, though its CD is 10 times smaller. The combination of ultra-low nonlinearity and dispersion enable operation at high optical powers and reduces the DSP-generated latency.

B. ARF-based long-haul transmission

Current HC-ARF research is focused on reducing the fiber attenuation and increasing the fiber length. Recent work has demonstrated a HC-ARF with less than 1.5 dB/km attenuation over 65 nm [22]. In our simulation, we investigate the performance of HC-ARF in long-reach coherent communications by considering 15 channels of 50 GBd Nyquist-shaped DP-16QAM signals. The optical channels centered at 1550 nm with a 100 GHz channel spacing. The effective nonlinear coefficient (γ) of the HC-ARF was assumed to be 0.01 $W^{-1}km^{-1}$ [33]. The in-line EDFAs were assumed to have 30 dB gain and a 7 dB noise figure.

Fig. 8 shows the simulated SNRs of the center channel with respect to different fiber attenuation values after transmission over a 1200 km HC-ARF link. The corresponding span length for different fiber attenuation levels is depicted as the upper-x axis. Different markers are used to indicate the SNRs at launch powers of 20 (square), 22 (circle), 24 (triangle), and 26 (diamond) dBm. Since the launch powers are significantly lower than those used in the experiment, we assume there is no

This work is licensed under a Creative Commons Attribution 3.0 License. For more information, see http://creativecommons.org/licenses/by/3.0/.

This article has been accepted for publication in a future issue of this journal, but has not been fully edited. Content may change prior to final publication. Citation information: DOI 10.1109/JLT.2018.2883541, Journal of Lightwave Technology

nonlinearity in the EDFAs. As a result, the signal performance is limited mainly by the amplified spontaneous emission (ASE) noise of the EDFAs.

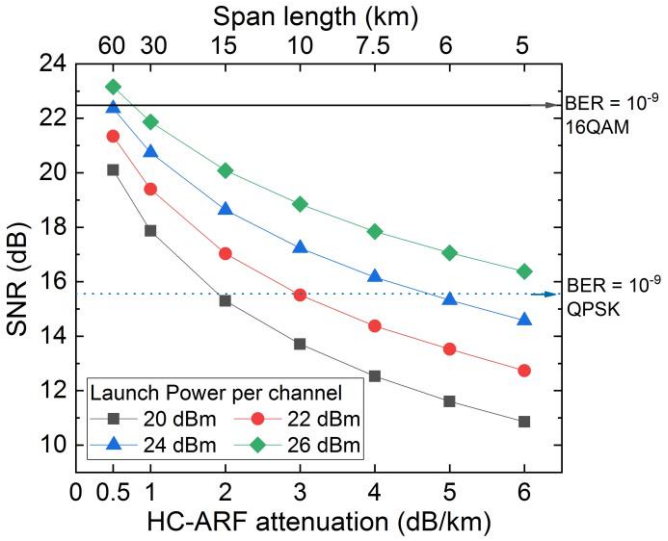

Fig. 8. Simulation results. Center channel SNR of the 15-channel WDM transmission over 1200 km HC-ARF link at launch powers of 20 (black square), 22 (red circle), 24 (blue triangle), and 26 dBm (green diamond).

The solid line shows the forward error correction (FEC) free SNR (22.5 dB) required for DP-16QAM signal transmission over the simulated link to achieve a BER of 10^{-9} (under the assumption of Additive White Gaussian Noise, AWGN), which indicates that the system can support FEC-free operation with a fiber attenuation of 0.77 dB/km when the launch power is higher than 26 dBm, achieving a data rate of 400 Gb/s per channel after 31 spans (39 km per span). The required SNR threshold FEC-free QPSK (15.6 dB, BER of 10^{-9}) are also shown in Fig. 8 as the dotted blue line. It shows that the system can achieve a net rate of 200 Gb/s even with 6 dB/km loss HC-ARF when the launch power to each span is higher than 26 dBm. Obviously, if the loss of HC-ARF can be reduced below 1 dB/km, the system can readily support FEC-free transmission at a launch power of around 16 dBm with a relatively low number of spans.

Although it is possible to achieve high throughput transmission using high attenuation HC-ARF, it would be at a high system cost and power consumption due to the large number of spans. However, the recently demonstrated 1.3 dB/km low loss HC-ARF (together with the theoretical predictions of even up to two orders of magnitude lower loss) show the potential of employing HC-ARF in long-haul communications. Such systems have an unprecedented advantage of low latency. For example, assuming a 40 m fiber length in each EDFA and a DSP processing latency of 20 µs, a 1200 km transmission link with 240 spans (considering 6 dB/km fiber attenuation) would have a latency of about 4.1 ms, which is 1.9 ms lower than that of an equivalent-length SMF-28 based transmission link. Similarly, for a 100 km link, a HC-ARF based system would have a latency of about 340 µs, providing a 150 µs reduction relative to SMF-28. In addition to the latency reduction, the hollow core fiber would have a more stable latency due to its significantly lower thermal coefficient [34], which benefits system stability in latency-sensitive real-time applications.

VI. Conclusion

We have presented 6.8 Tb/s coherent data transmission over 270 m of HC-ARF. The excellent quasi single mode behavior of the fiber allowed us to transmit dual-polarization-256QAM signals in a coherent 16-channel WDM system with negligible SNR penalty, and to achieve the highest data rate transmitted through an HC-ARF to date. We have also experimentally confirmed that the fiber can handle high optical powers (up to 36.5 dBm, giving it 2 dB SNR advantage over SMF-28 in a comparison that is deliberately biased against the HC-ARF, using a power after transmission of up to 28.5 dBm. Our simulations show that HC-ARF has a clear advantage over different types of solid core fibers in terms of insensitivity to nonlinearities, even though its CD is significantly smaller. These results, together with inherently lower and more stable latency and potential for significant further loss reduction make HC-ARF a most promising transmission medium for future low-latency, ultra-high capacity data transmission applications.

References

[1] R. J. Essiambre et al., "Capacity limits of optical fiber networks," *IEEE/OSA J. Lightwave Technol.*, vol. 28, no. 4, pp. 662–701, 2010.

[2] M. M. Filer, S. Searcy, Y. Fu, R. Nagarajan, and S. Tibuleac, "Demonstration and Performance Analysis of 4 Tb/s DWDM Metro-DCI System with 100G PAM4 QSFP28 Modules," *in Proc. OFC, paper W4D.4*, 2017.

[3] M. Simsek, A. Aijaz, M. Dohler et al., "5G-Enabled Tactile Internet," vol. 34, no. 3, pp. 460-473, 2016.

[4] E. Ip, "Nonlinear compensation using backpropagation for polarization-multiplexed transmission," *IEEE/OSA J. Lightwave Technol.*, vol. 28, no. 6, pp. 939-951, 2010.

[5] S. K. Turitsyn *et al.*, "Nonlinear Fourier transform for optical data processing and transmission: advances and perspectives," *Optica*, vol. 4, no.3, 2017.

[6] S. Yoshima *et al.*, "Mitigation of Nonlinear Effects on WDM QAM Signals Enabled by Optical Phase Conjugation with Efficient Bandwidth Utilization," *IEEE/OSA J. Light. Technol.*, vol. 35, no. 4, pp. 971–978, 2017.

[7] R. Slavík *et al.*, "All-optical phase and amplitude regenerator for next-generation telecommunications systems," *Nat. Photonics*, vol. 4, pp. 690–695, 2010.

[8] S.L.I. Olsson et al., "Long-haul optical transmission link using low-noise phase-sensitive amplifiers," vol. 9, no. 2513, 2018.

[9] S. Kametani, T. Sugihara, T. Kobayashi et al., "Low latency Transmission at 40 Gbps by Employing Electronic Pre-equalization Techonlogy," in Proc. OFC, paper OThE2, 2011.

[10] GTT Network. https://www.gtt.net/services/transport-services/low-latency/

[11] Y. Sagae, T. Matsui, K. Tsujikawa, K. Nakajima, "Solid Type Low-Latency Single-Mode Fiber with Large Effective Area and Low loss," in Proc. OFC, paper Th2A.27, 2018.

[12] F. Poletti, N.V. Wheeler, M.N. Petrovich *et al.*, "Towards high-capacity fibre-optic communications at the speed of light in vacuum," *Nat. Photonics*, vol. 7, pp. 279-284, 2013.

[13] S.A. Mousavi, H.C.H. Mulvad, N.V. Wheeler et al., "Nonlinear dynamic of picosecond pulse propagation in atmospheric air-filled hollow core fibers," *Opt. Express*, vol. 26, no. 7, pp. 8866-8882, 2018.

[14] F. Poletti M.N. Petrovich, D.J. Richardson, "Hollow-core photonic bandgap fibers: technology and applications," Nanophotonics, vol. 2, no.5-6, pp. 315–340, pp. 315-340. 2013.

[15] J.R. Hayes et al., "Antiresonant Hollow Core Fiber with an Octave Spanning Bandwidth for Short Haul Data Communications," *IEEE/OSA J. Lightw. Technol*, vol. 35, no., pp. 437-442, 2017.

This work is licensed under a Creative Commons Attribution 3.0 License. For more information, see http://creativecommons.org/licenses/by/3.0/.

This article has been accepted for publication in a future issue of this journal, but has not been fully edited. Content may change prior to final publication. Citation information: DOI 10.1109/JLT.2018.2883541, Journal of Lightwave Technology

[16] P. Uebel et al., "Broadband Robustly Single-mode Hollow-Core PCF by Resonant Filtering of Higher-order Modes," *Opt. Lett.*, vol. 41, no. 9, pp. 1961–1964, 2016.
[17] F. Yu et al., "Experimental Study of Low-loss Single-mode Performance in Anti-resonant Hollow-core Fibers," *Opt Express*, vol. 24, no.12, pp. 12969-12975, 2016.
[18] B. Debord, et al. "Ultralow Transmission Loss in Inhibited-coupling Guiding Hollow Fibers," *Optica*, vol. 4, no.2, pp. 209-217, 2017.
[19] F. Poletti, "Nested Antiresonant nodeless hollow core fiber," *Opt. Express*, vol. 22, no. 20, pp. 23807-23828, 2014.
[20] V. A. J. M. Sleiffer et al., "High Capacity Mode-Division Multiplexed Optical Transmission in a Novel 37-cell Hollow-Core Photonic Bandgap Fiber," *IEEE/OSA J. Lightw. Technol.*, vol. 32, no.4, pp. 854–863, 2014.
[21] M. Kuschnerov et al., "Data Transmission Through up to 74.8 km of Hollow-Core Fiber with Coherent and Direct-Detect Transceivers," *in Proc. ECOC*, paper Th1.2.4, 2015.
[22] T.D. Bradley et al., "Record Low-Loss 1.3dB/km Data Transmitting Antiresonant Hollow Core Fibre," *in Proc. ECOC*, paper Th3F.2, 2018.
[23] B.J. Mangan et al., "Low loss (1.7 dB/km) hollow core photonic bandgap fiber," *in Proc. OFC.*, paper PD24, 2004.
[24] Z. Liu et al., "Record high capacity (6.8 Tbit/s) WDM coherent transmission in hollow-core antiresonant fiber," *in Proc. OFC*, paper Th5B.8, 2017.
[25] T. Niemi, M. Uusimaa, and H. Ludvigsen, "Limitations of phase-shift method in measuring dense group delay ripple of fiber Bragg gratings," *IEEE Photonics Technol. Lett.*, vol. 13, no.12, pp. 1334-1336, 2001.
[26] B. Tatian, "Fitting refractive-index data with the Sellmeier dispersion formula," *Applied Optics*, vol. 23, no. 23, pp. 4477-4485, 1984.
[27] S.J. Savory, "Digital filters for coherent optical receivers," *Opt. Express*, vol. 16, no. 2, pp. 804-817, 2008.
[28] Y. Chen, Z. Liu, S.R. Sandoghchi et al., "Multi-kilometer Long, Longitudinally Uniform Hollow Core Photonic Bandgap Fibers for Broadband Low Latency Data Transmission," *OSA/IEEE J. Lightw. Technol.*, vol. 34, no. 1, pp. 104-113, 2016.
[29] R. Maher et al., "Increasing the Information Rates of Optical Communications via Coded Modulation: a Study of Transceiver Performance," *Scientific Report*, 6, pp. 21278, 2016.
[30] L. Galdino, D. Lavery, Z. Liu et al., "The Trade-off Between Transceiver Capacity and Symbol Rate," *in Proc. OFC*, paper W1B.4, 2018.
[31] S. Makovejs et al., "Record-low (0.1460 dB/km) Attenuation Ultra-Large Aeff Optical Fiber for Submarine Applications," in Proc. OFC, paper Th5A.2, 2015.
[32] Corning LEAF optical fiber product specification. https://www.corning.com/media/worldwide/coc/documents/Fiber/LEAF%20optical%20fiber.pdf
[33] Abokhamis Mousavi et al., "Nonlinear dynamic of picosecond pulse propagation in atmospheric air-filled hollow core fibers," Opt. Express, vol.26, no.7, pp.8866-8882, 2018.
[34] Radan Slavík, Giuseppe Marra, Eric Numkam Fokoua, et al., "Ultralow thermal sensitivity of phase and propagation delay in hollow core optical fibres," Scientific Report, vol. 5, no. 15447, 2015.

This work is licensed under a Creative Commons Attribution 3.0 License. For more information, see http://creativecommons.org/licenses/by/3.0/.